Impact on the tensor-to-scalar ratio of foreground mismodelling for future CMB satellites

Mathieu Remazeilles

MANCHESTER 1824

The University of Manchester

Remazeilles, M., Dickinson, C., Eriksen, H.K.K., Wehus, I.K.
MNRAS (2016)

EWASS 2016
Athens, 4-8 July 2016

Big Bang gravitational waves from inflation?

Hu et al 2003

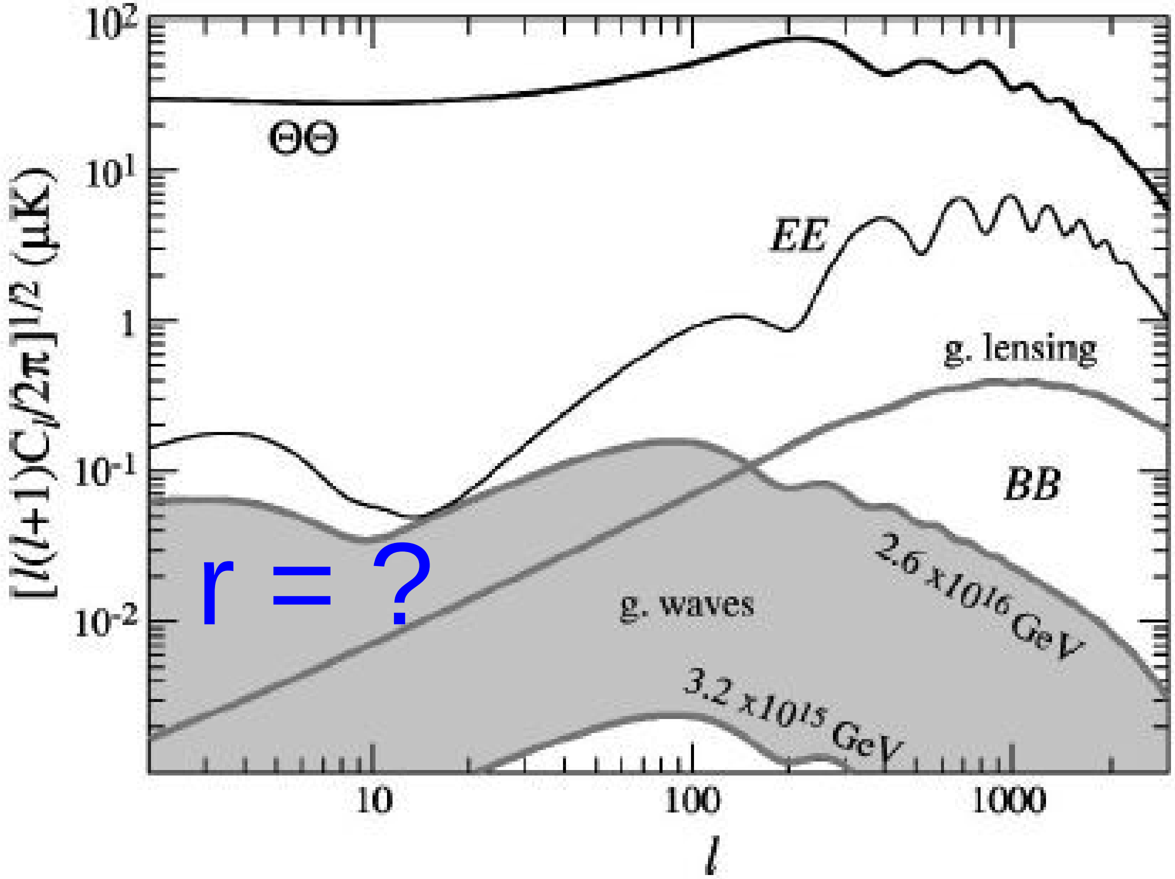

- CMB B-mode polarization predicted by inflation
- Tensor-to-scalar ratio **r** : amplitude of CMB B-mode angular power spectrum
- **r** determines the energy scale of inflation: $\boldsymbol{r = 0.008 \times (E_{inf} / 10^{16}\ GeV)^{4}}$

Future CMB satellites all aim at detecting r ~ 0.001

LiteBIRD

Matsumura et al., 2013

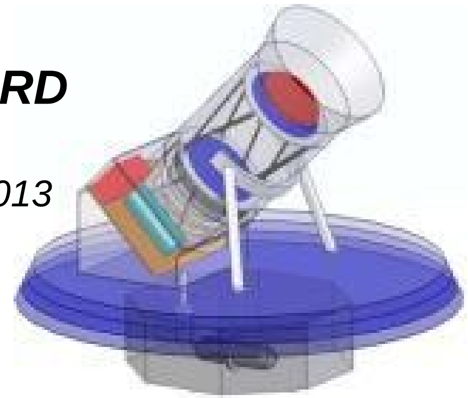

COrE

COrE Collaboration et al., 2011

Kogut et al., 2011

Bock et al., 2008

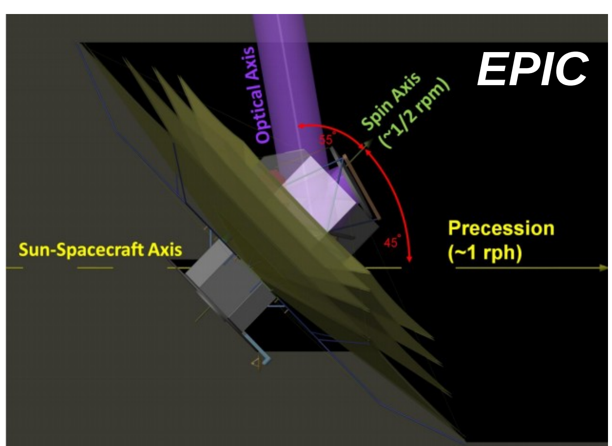

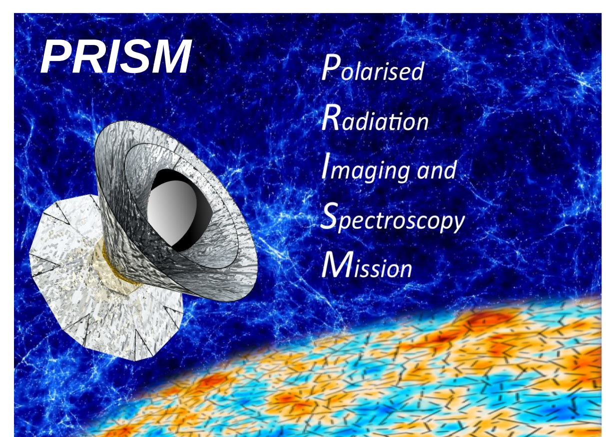

André et al., 2014

Sensitivity of B-mode satellite concepts

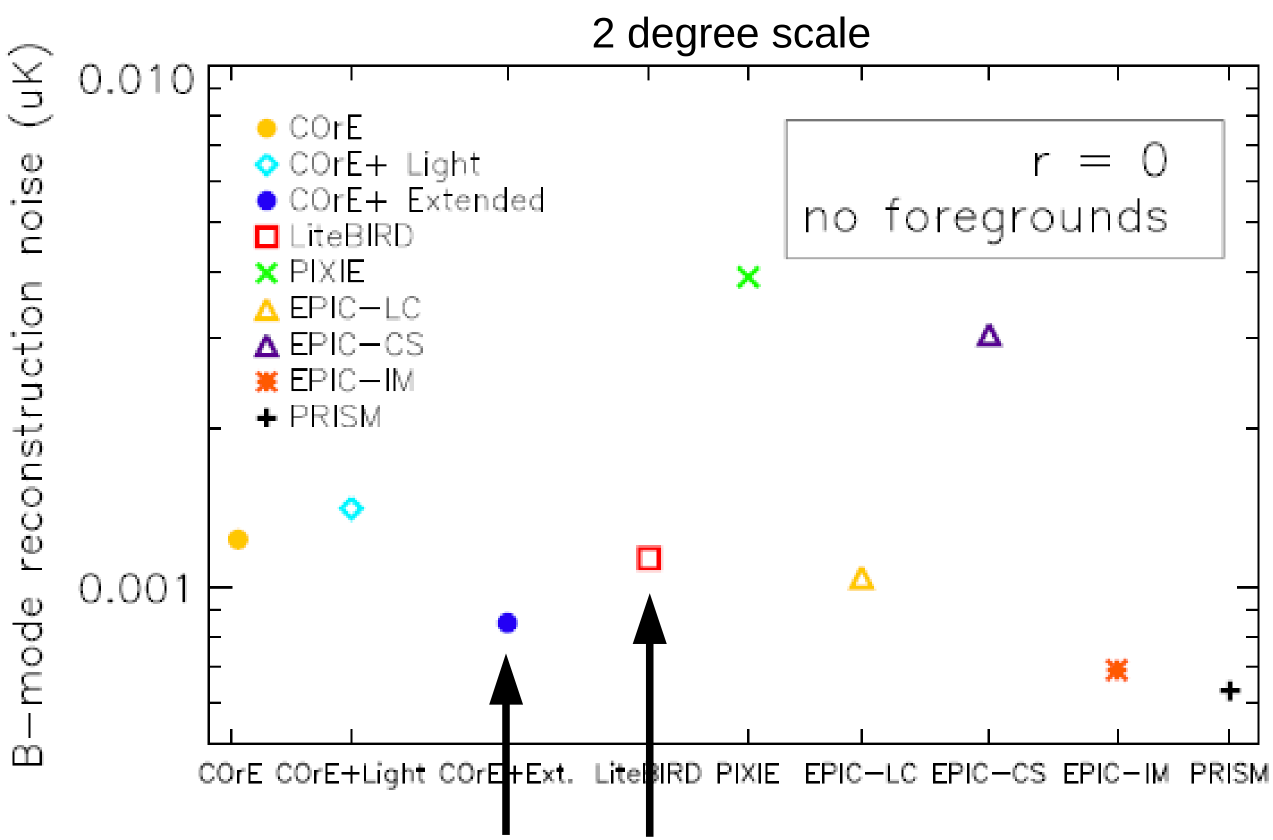

COrE+ **LiteBIRD**

Increase in sensitivity

$1 / \sigma_{eff}^2 = \sum_i 1 / \sigma_i^2$

« Because of much larger sensitivity of future CMB space missions, the estimation of the tensor-to-scalar ratio will be much more sensitive to imperfect foreground modelling »

Remazeilles, Dickinson, Eriksen, Wehus, MNRAS 2016

Astrophysical foregrounds

Errard et al 2016

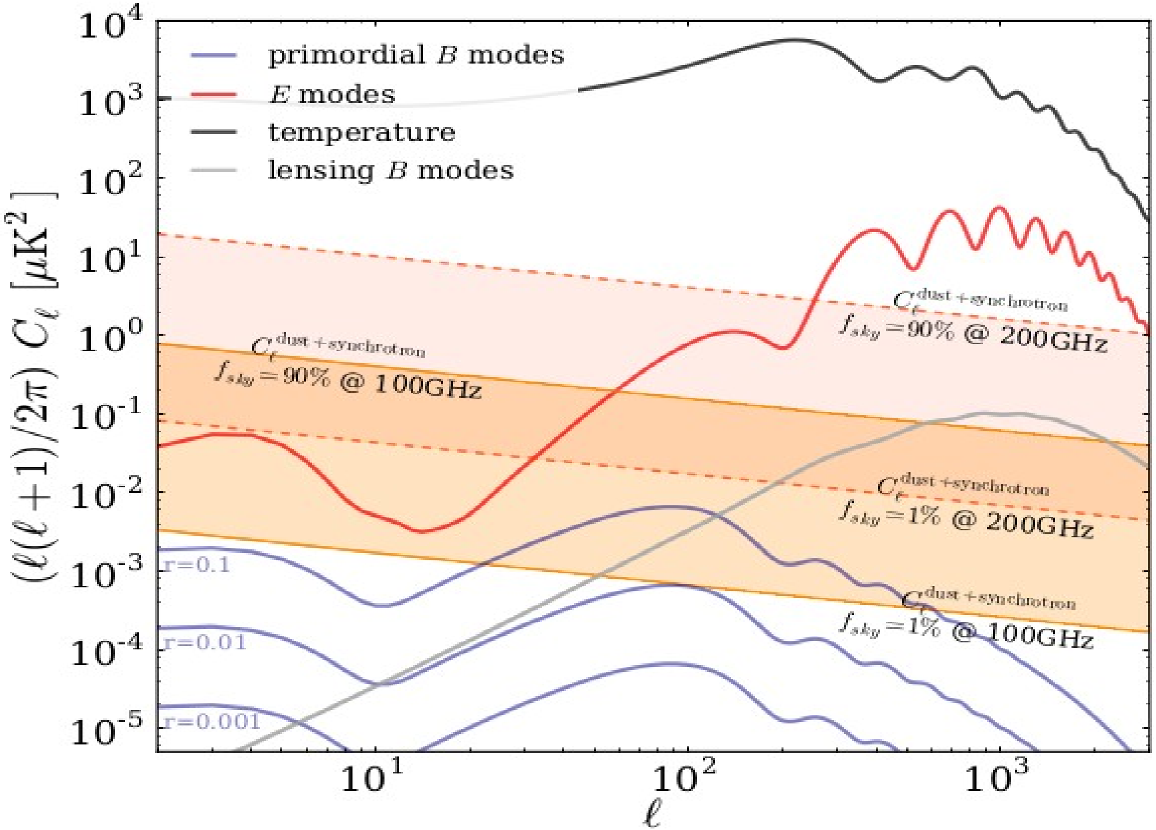

- Foregrounds = everything between last scattering surface and detectors
- At any frequency, any direction of the sky, any angular scale:
  Galactic foregrounds much more polarized than CMB, by many orders of magnitude!

Large scale polarized foregrounds

Component	***Spectrum***	***Polarization fraction***	***References***
Synchrotron	*- Power-law $\beta\sim-3$, variations $\Delta\beta\sim0.2$* *- In theory, curvature C=-0.3* *- Flattening from multiple power-laws / populations of electrons*	*~15-20%* *(up to ~50%)*	*Page et al (2007), Kogut et al (2007), Macellari et al (2011)* *Vidal et al (2015)*
Thermal dust	*- Modified black-body* *- Possibly 2 components/flattening* *at frequencies <300 GHz*	*~5% - 10%* *(up to ~20+%)*	*Ponthieu et al (2005), Planck Collaboration, ESLAB conference (2013).* *Planck intermediate results. XIX*
Magnetic dipole?	*- Similar to thermal dust, but flatter index at frequencies ~100 GHz* *- Not yet detected (70GHz-300 GHz)*	*Variable* *(up to ~35% ?)* *<~5%*	*Draine & Lazarian (1999), Draine & Hensley (2013)* *Hoang & Lazarian (2015)*
spinning dust	*- Peaked spectrum ~10-60 GHz*	*<~1%* *Perseus:0.6+/-0.5%*	*Lazarian & Draine (2000), Dickinson (2011), Lopez-Caraballo et al. (2011), Macellari et al. (2011), Rubino-Martin et al. (2012)* *Planck 2015 results. XXV*
Free-free	*- Power-law $\beta\sim-2.14$ with positive curvature (steepening at frequencies >~100 GHz)*	*Intrisically zero,* *in practice <~1%*	*Rybicki & Lightman (1979), Keating et al. (1998), Macellari et al. (2011)*

Example: synchrotron radiation

WMAP 9-year 23 GHz polarised intensity

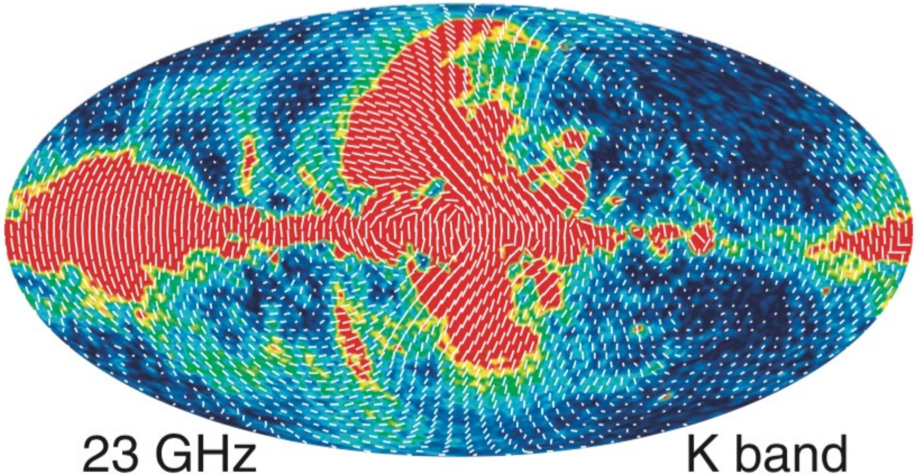

Bennett et al. 2013

Synchrotron polarisation fraction

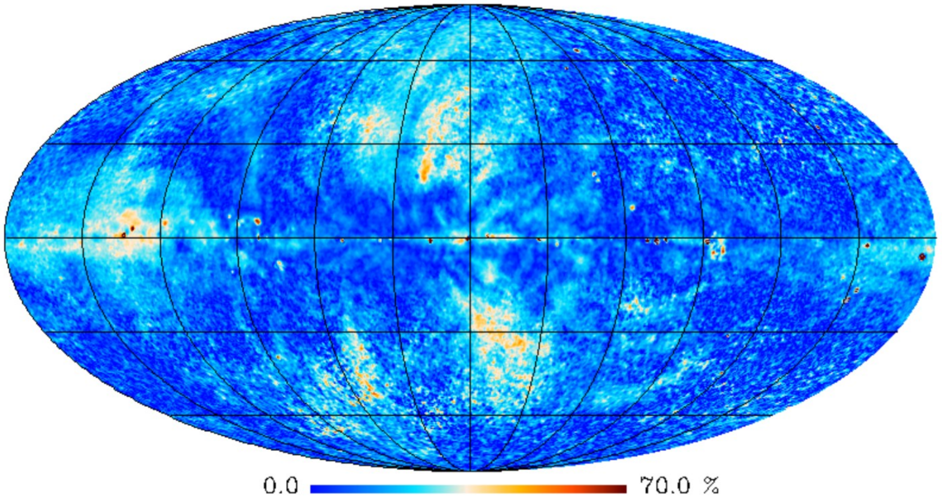

Planck Collaboration, 2015, arXiv:1506.06660

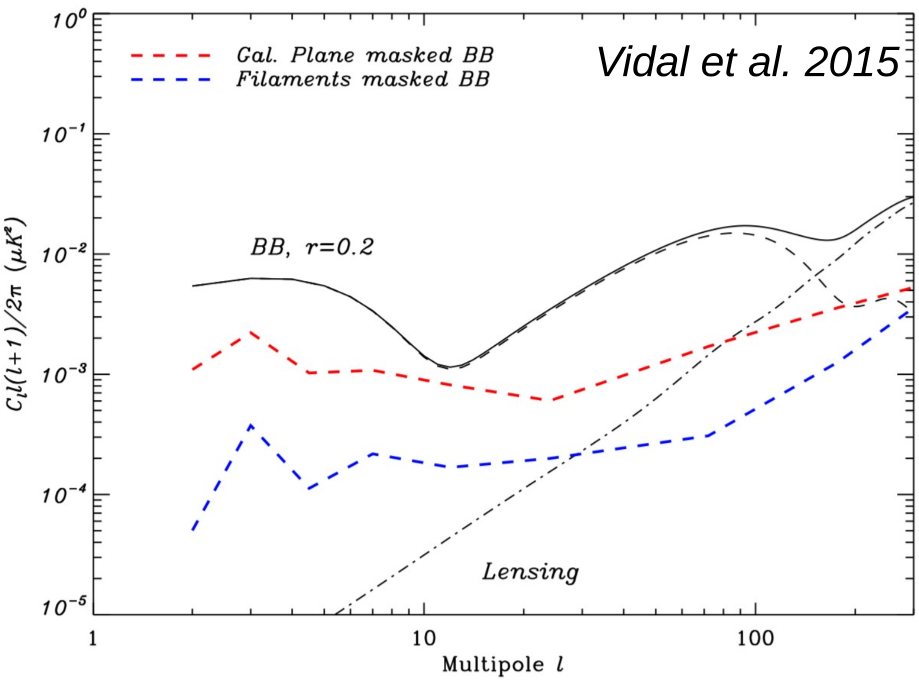

- Up to 70% polarized
- Large filaments outside Galactic plane responsible for the bulk of synchrotron

galactic masking won't help that much !

Example: uncertainties on spectral indices

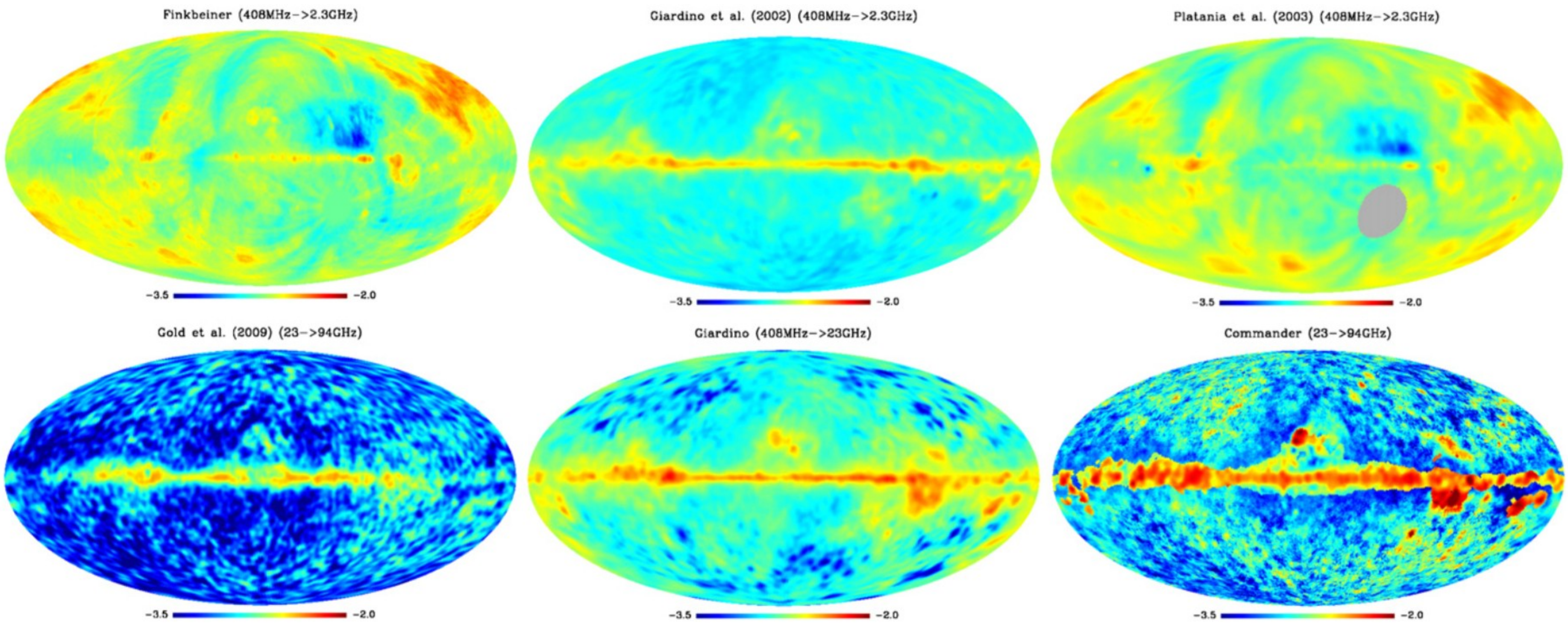

Dickinson et al 2009

- **Synchrotron spectral indices are not very accurate**
  Low frequencies: data quality (systematics)
  High frequencies: component separation

- **Significant variations over the sky**

Even more uncertainties on foregrounds

- Synchrotron : what is the curvature of the spectral index ?
- Thermal dust : how many greybodies ?
- Spinning dust : 1% polarization might be significant for r=0.001 given the sensivity of future CMB experiments ?
- Magnetic dust : can be up to 35% polarized in theory but no observation so far
  Blackbody-like spectrum at 70-100 GHz → a killer for CMB B-modes !

Even more uncertainties on foregrounds

- Synchrotron : what is the curvature of the spectral index ?
- Thermal dust : how many greybodies ?
- Spinning dust : 1% polarization might be significant for r=0.001 given the sensivity of future CMB experiments ?
- Magnetic dust : can be up to 35% polarized in theory but no observation so far
  Blackbody-like spectrum at 70-100 GHz → a killer for CMB B-modes !

B-mode component separation is challenging !

Bayesian parametric fitting

COMMANDER - Eriksen et al (2008)

Parametric model of the sky

$$\mathbf{m}(p,\nu) = a(\nu)\,\mathbf{s}^{cmb}(p) + \left(\frac{\nu}{\nu_0^s}\right)^{\beta_s(p)} \mathbf{s}^{sync}(p) + \left(\frac{\nu}{\nu_0^d}\right)^{\beta_d(p)} B_\nu\left(T_d(p)\right)\mathbf{s}^{dust}(p) + \mathbf{n}(p,\nu)$$

Fit spectral model to data pixel by pixel

Joint CMB-foreground posterior ?

$$P\left(s,\beta,C_\ell \middle| d\right) \propto P\left(d \middle| s,\beta,C_\ell\right) P\left(s,\beta,C_\ell\right)$$

COMMANDER methodology

Eriksen et al, ApJ 2008
Remazeilles et al, MNRAS 2016

1. Separation of components (MCMC Gibbs sampling)

$$s^{(i+1)} \leftarrow P\left(s \middle| C_\ell^{(i)}, \beta^{(i)}, d\right),$$ amplitudes

$$C_\ell^{(i+1)} \leftarrow P\left(C_\ell \middle| s^{(i+1)}\right),$$ CMB power spectrum

$$\beta^{(i+1)} \leftarrow P\left(\beta \middle| s^{(i+1)}, d\right),$$ spectral indices

2. Likelihood estimation of r :

$$-2\ln\mathcal{L}\left[\widehat{C}_\ell | C_\ell^{th}\left(r, A_{lens}\right)\right] = \sum_\ell (2\ell+1)\left[\ln\left(\frac{C_\ell^{th}}{\widehat{C}_\ell}\right) + \frac{C_\ell^{th}}{\widehat{C}_\ell} - 1\right]$$

$$C_\ell^{th} = r\, C_\ell^{tensor}(r=1) + A_{lens}\, C_\ell^{lensing}(r=0).$$

Blackwell-Rao: $P(r) = \sum_{\text{Gibbs samples (i)}} \mathcal{L}\left[\hat{C}_\ell^{(i)} \mid C_\ell^{th}(r)\right]$

COMMANDER output examples

CMB Q INPUT

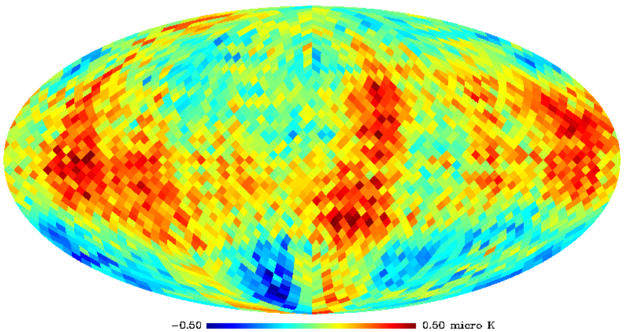

CMB Q COMMANDER

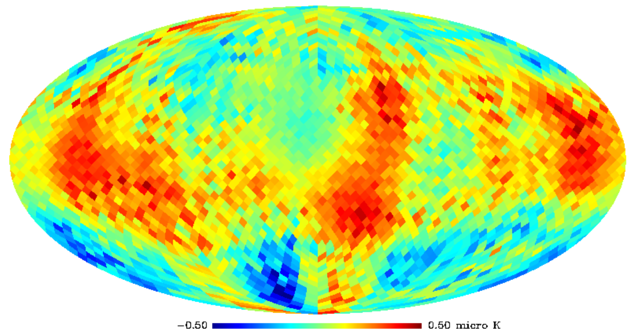

CMB RESIDUALS

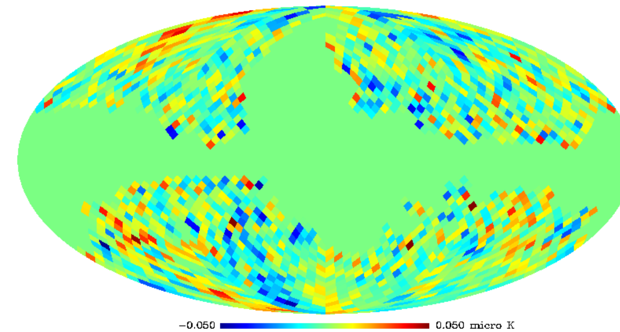

Dust β COMMANDER

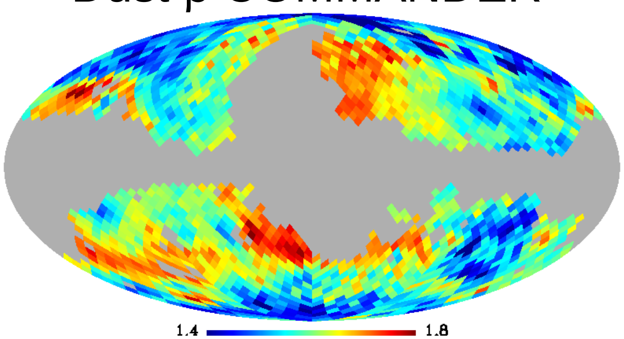

Dust T COMMANDER

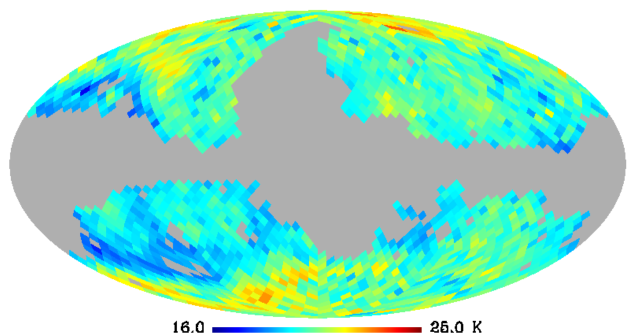

Synchrotron β COMMANDER

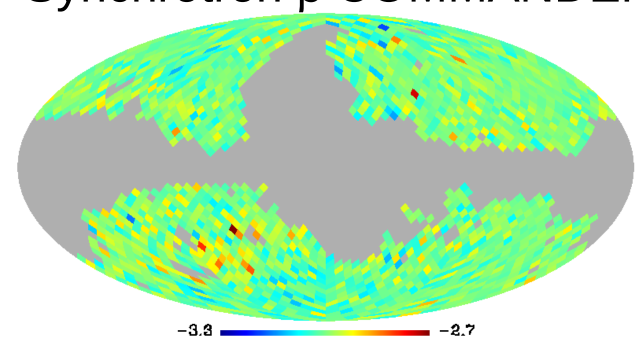

CHI-SQUARE

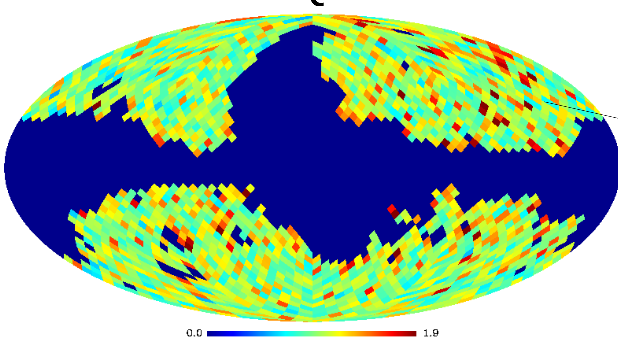

χ^2 goodness-of-fit over the sky

(i) gives feedback on foreground modelling

(ii) tells where to mask a posteriori

Impact of foreground mismodelling ?

mismatch between foreground model and real data

$$\begin{aligned}\boldsymbol{m}(p,\nu) &= a(\nu)\,\boldsymbol{s}^{cmb}(p)\\ &+ \left(\frac{\nu}{\nu_0^s}\right)^{\beta_s(p)} \boldsymbol{s}^{sync}(p)\\ &+ \left(\frac{\nu}{\nu_0^d}\right)^{\beta_d(p)} B_\nu\left(T_d(p)\right)\boldsymbol{s}^{dust}(p)\\ &+ \boldsymbol{n}(p,\nu)\end{aligned}$$

Model

$$\begin{aligned}\boldsymbol{d}(p,\nu) &= a(\nu)\,\boldsymbol{s}^{cmb}(p)\\ &+ \left(\frac{\nu}{\nu_0^s}\right)^{\beta_s(p)+C\ln(\nu/\nu_0^s)} \boldsymbol{s}^{sync}(p)\\ &+ \left[f_1\left(\frac{\nu}{\nu_0^d}\right)^{\beta_1(p)} B_\nu\left(T_1(p)\right)+f_2\left(\frac{\nu}{\nu_0^d}\right)^{\beta_2(p)} B_\nu\left(T_2(p)\right)\right]\boldsymbol{s}^{dust}(p)\\ &+ \epsilon(\nu)\,\boldsymbol{s}^{spinning\ dust}(p)\\ &+ \boldsymbol{n}(p,\nu)\end{aligned}$$

synchrotron curvature

extra thermal dust

spinning dust

Data

Remazeilles, Dickinson, Eriksen, Wehus, *MNRAS 2016*

Perfect foreground modelling

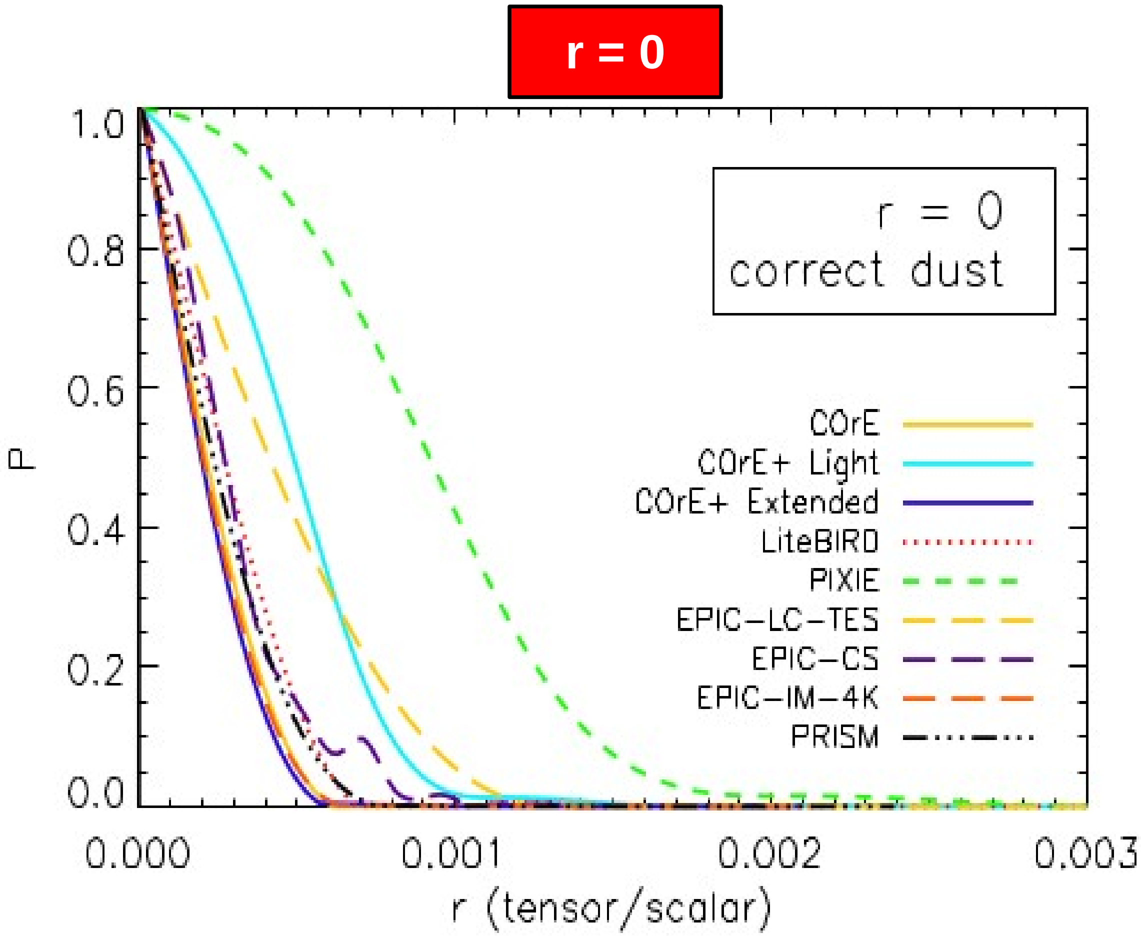

$\ell_{max} \sim 12$

χ^2	r	
1.00	0.00031 ± 0.00024	COrE+ Light
0.99	0.00016 ± 0.00012	COrE+ Extended
0.99	0.00017 ± 0.00013	COrE
0.99	0.00020 ± 0.00017	LiteBIRD
0.99	0.00056 ± 0.00042	PIXIE
1.06	0.00033 ± 0.00026	EPIC-LC-TES
0.97	0.00023 ± 0.00020	EPIC-CS
0.98	0.00016 ± 0.00013	EPIC-IM-4K
0.99	0.00019 ± 0.00015	PRISM

Remazeilles, Dickinson, Eriksen, Wehus, MNRAS 2016

Impact of mismodelling dust: omitting one greybody component

r = 0

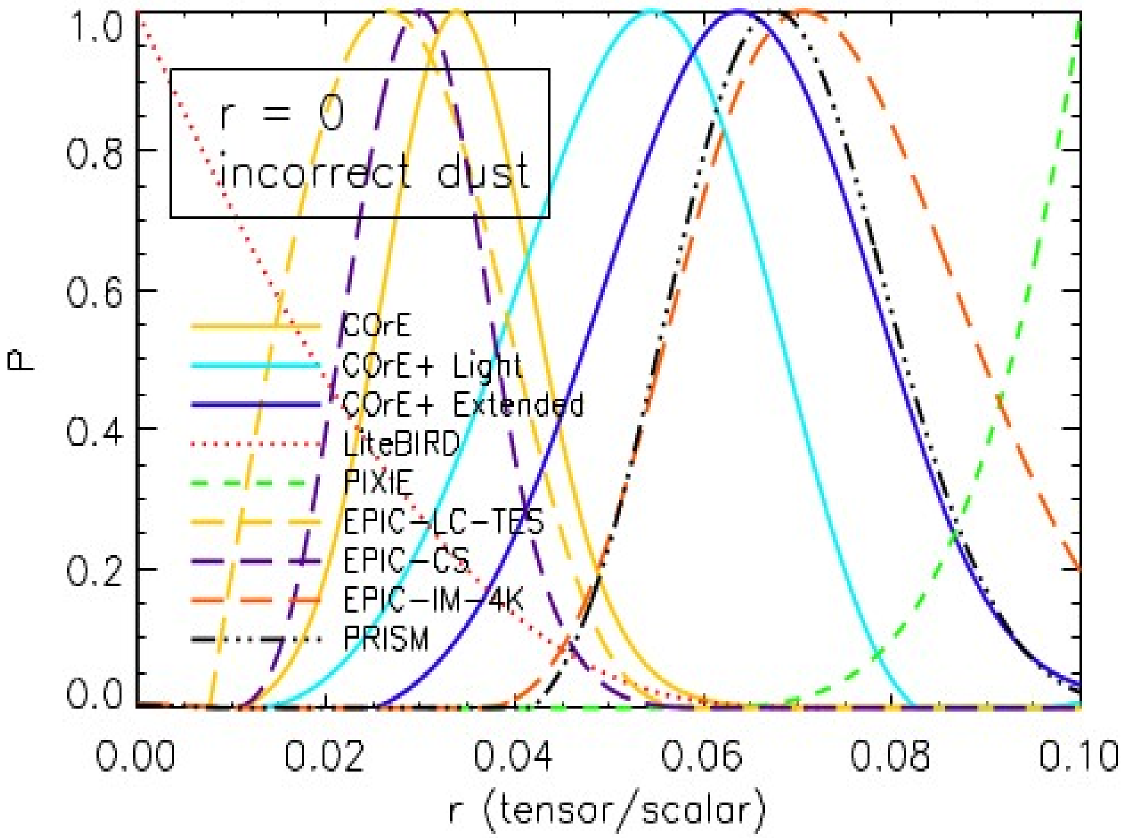

Incorrect spectral modelling of thermal dust strongly bias the most sensitive experiments

$\ell_{max} \sim 12$

χ^2	r	
1.07	0.05229 ± 0.01223	COrE+ Light
1.20	0.06357 ± 0.01332	COrE+ Extended
1.12	0.03453 ± 0.00821	COrE
1.10	0.01595 ± 0.01249	LiteBIRD
1.08	0.09246 ± 0.00635	PIXIE
1.33	0.02792 ± 0.00936	EPIC-LC-TES
1.08	0.03018 ± 0.00699	EPIC-CS
2.88	0.07251 ± 0.01265	EPIC-IM-4K
1.58	0.06885 ± 0.01068	PRISM

High-frequency channels very useful to highlight incorrect dust modelling

Remazeilles, Dickinson, Eriksen, Wehus, MNRAS 2016

Incorrect foreground modelling: a minor impact for Planck

Armitage-Caplan et al., MNRAS 2012

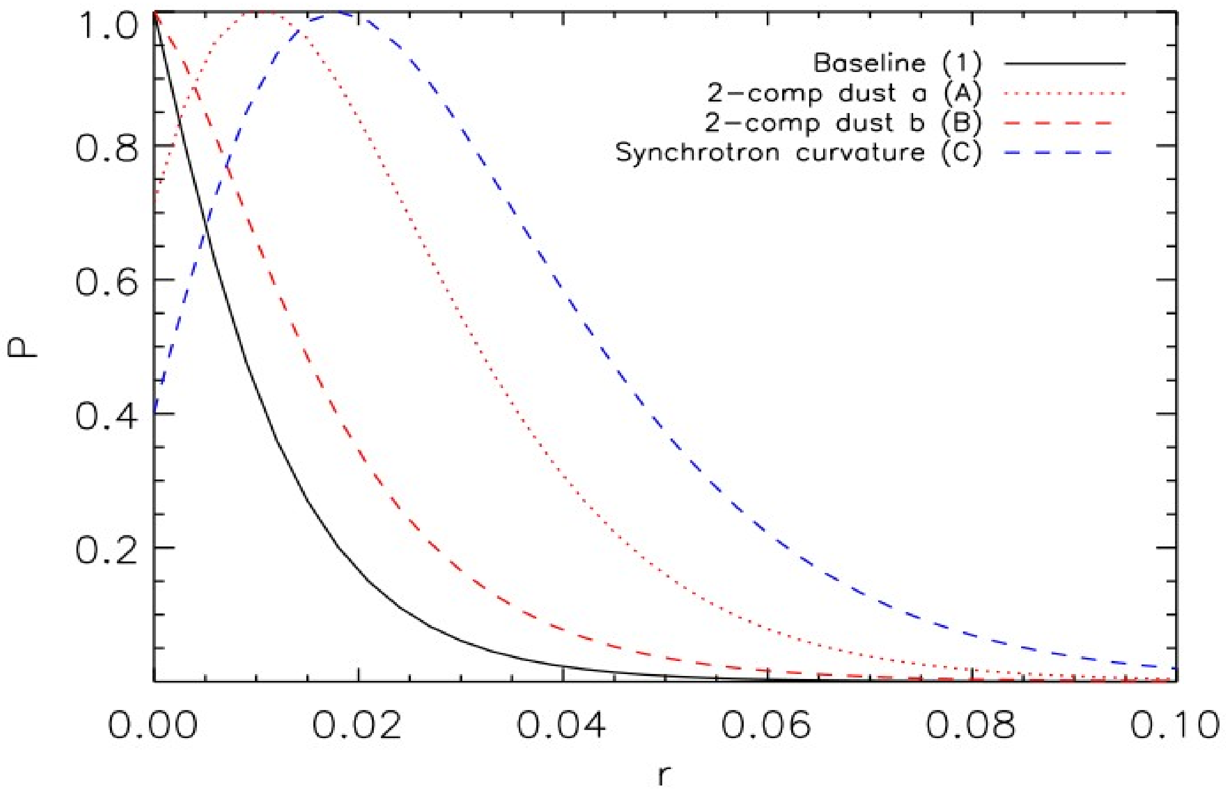

Because of lower sensitivity, <u>Planck is less impacted</u> by incorrect assumptions on the Galactic foreground spectral properties

Impact of missing faint polarized foregrounds: 1% polarized spinning dust

r = 0

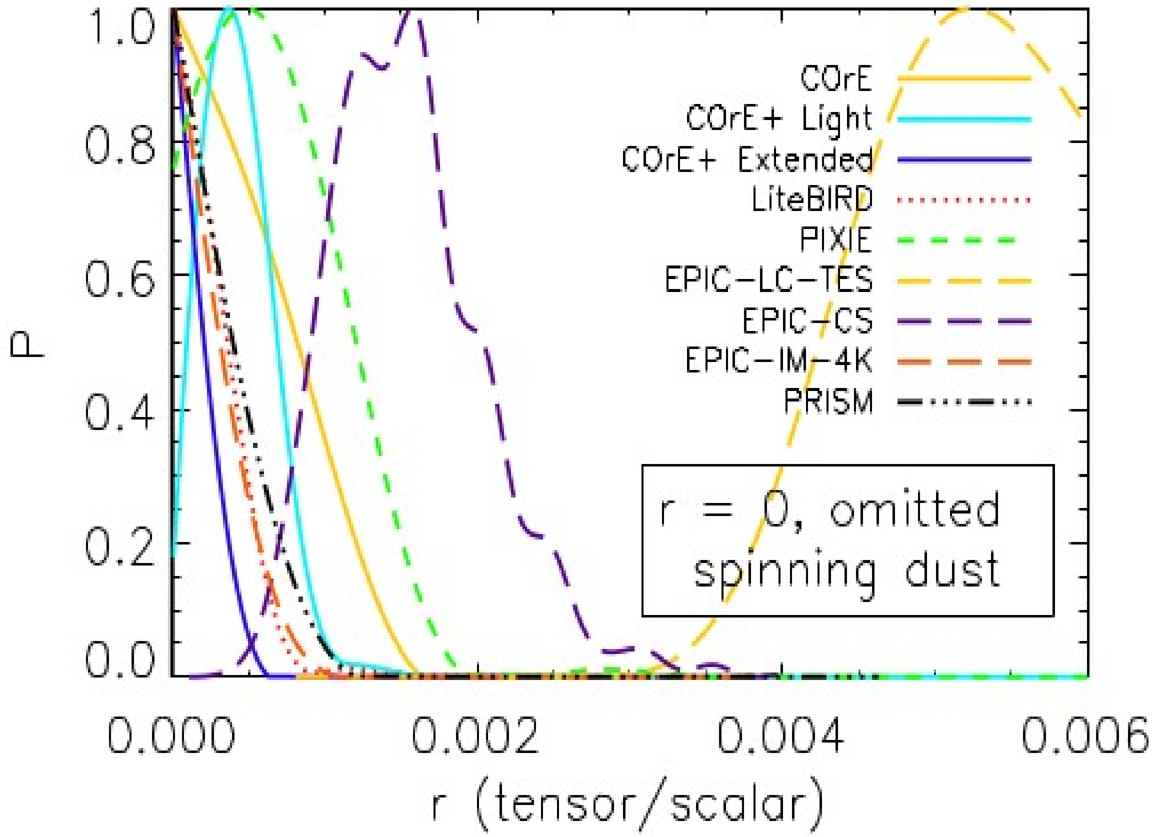

Omitting the 1% polarized spinning dust makes a ***non-negligible bias*** *on the tensor-to-scalar ratio for some experiments*

$\ell_{max} \sim 12$

Remazeilles, Dickinson, Eriksen, Wehus, MNRAS 2016

No foregrounds

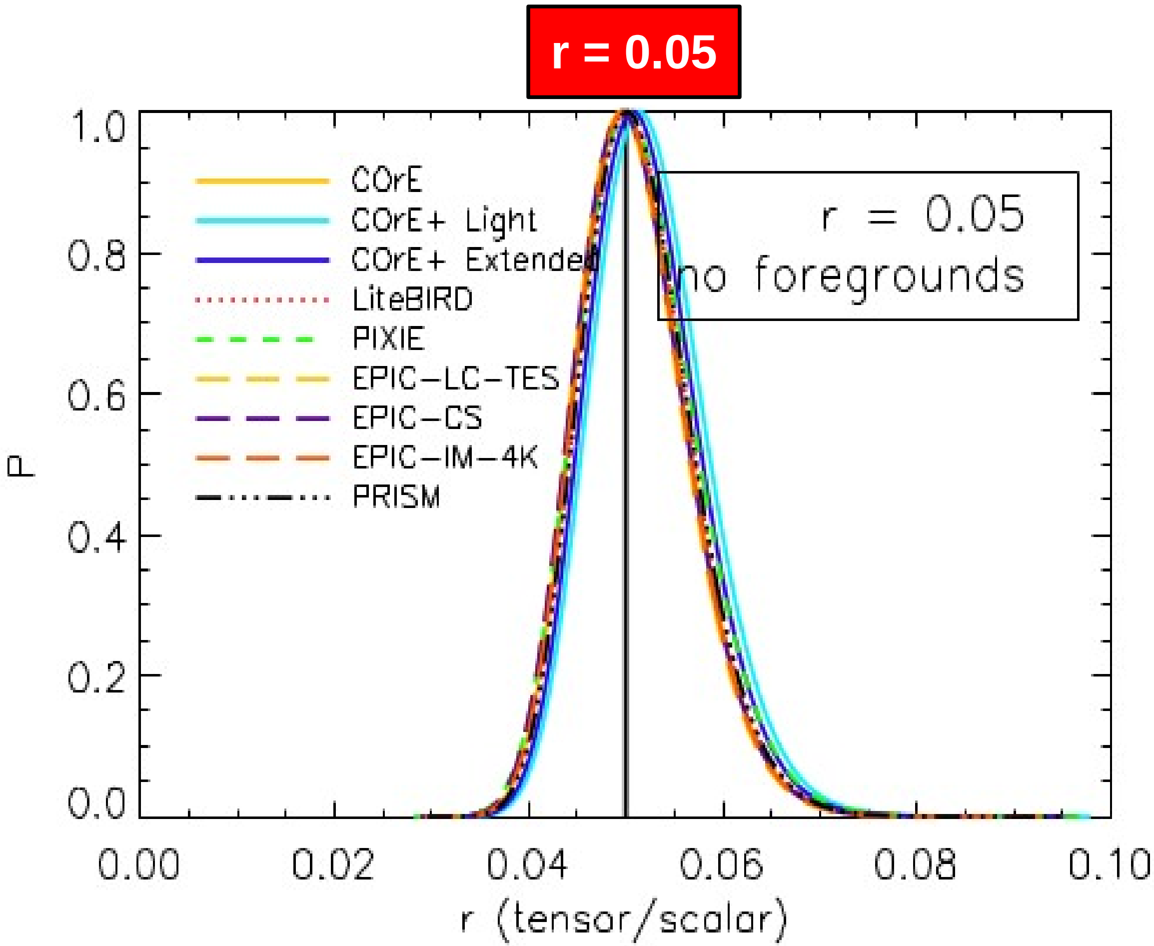

*errors on **r** dominated by cosmic variance for all satellite concepts*

$\ell_{max} \sim 12$

χ^2	r	
0.99	0.05271 ± 0.00595	COrE+ Light
0.99	0.05202 ± 0.00585	COrE+ Extended
0.98	0.05107 ± 0.00575	COrE
0.96	0.05132 ± 0.00578	LiteBIRD
0.99	0.05145 ± 0.00616	PIXIE
0.97	0.05074 ± 0.00572	EPIC-LC-TES
0.96	0.05086 ± 0.00583	EPIC-CS
0.97	0.05096 ± 0.00572	EPIC-IM-4K
0.99	0.05140 ± 0.00578	PRISM

9σ detection

9σ detection

Remazeilles, Dickinson, Eriksen, Wehus, MNRAS 2016

Foregrounds: perfect modelling

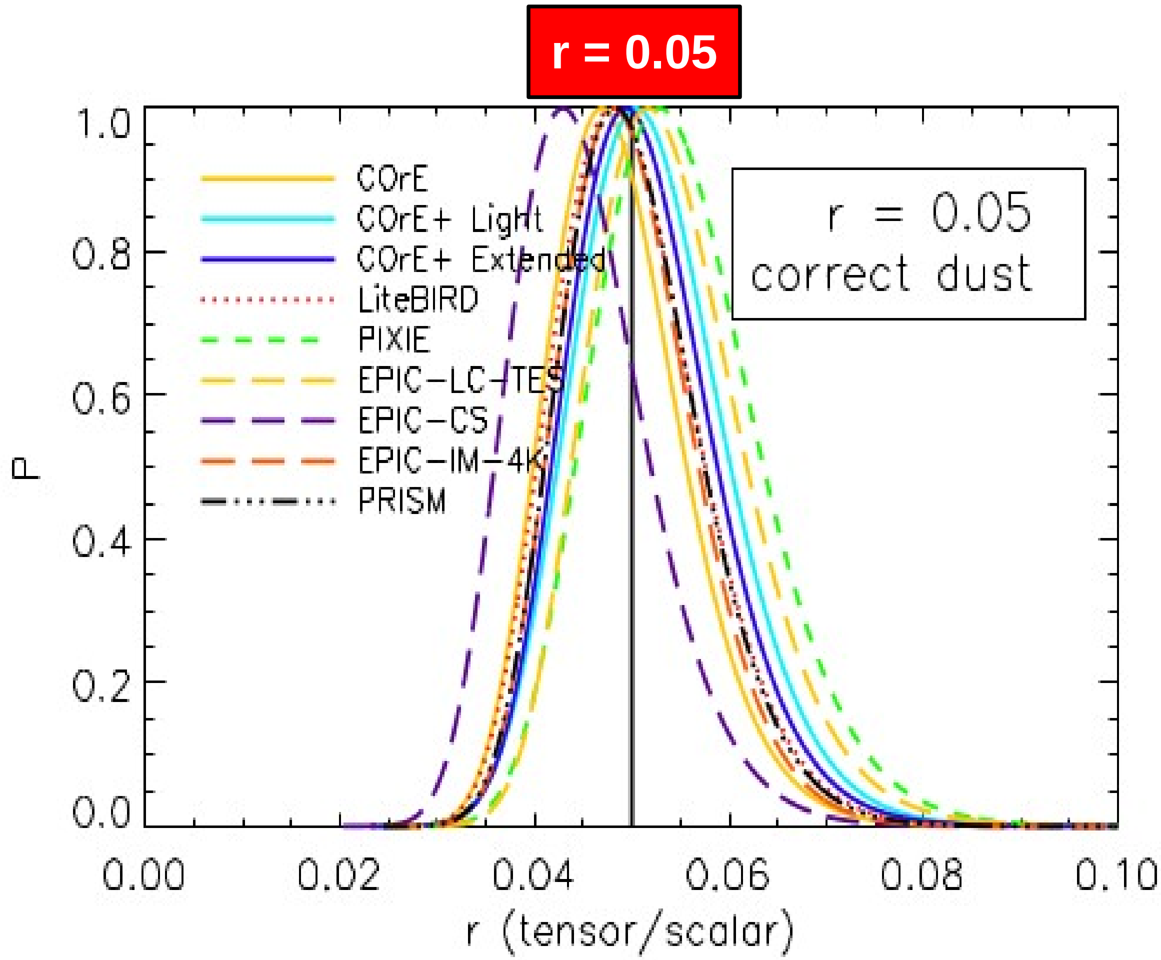

*Galactic foregrounds inflate the error on **r** but there is no bias*

$\ell_{max} \sim 12$

χ^2	r	
1.00	0.05224 ± 0.00800	COrE+ Light
0.99	0.05132 ± 0.00770	COrE+ Extended
0.99	0.04877 ± 0.00715	COrE
0.99	0.04997 ± 0.00767	LiteBIRD
1.00	0.05507 ± 0.00865	PIXIE
1.06	0.05411 ± 0.00823	EPIC-LC-TES
0.97	0.04506 ± 0.00730	EPIC-CS
0.98	0.04989 ± 0.00708	EPIC-IM-4K
1.00	0.05027 ± 0.00737	PRISM

7σ detection

6.5σ detection

Remazeilles, Dickinson, Eriksen, Wehus, MNRAS 2016

Impact of mismodelling dust: omitting one greybody component

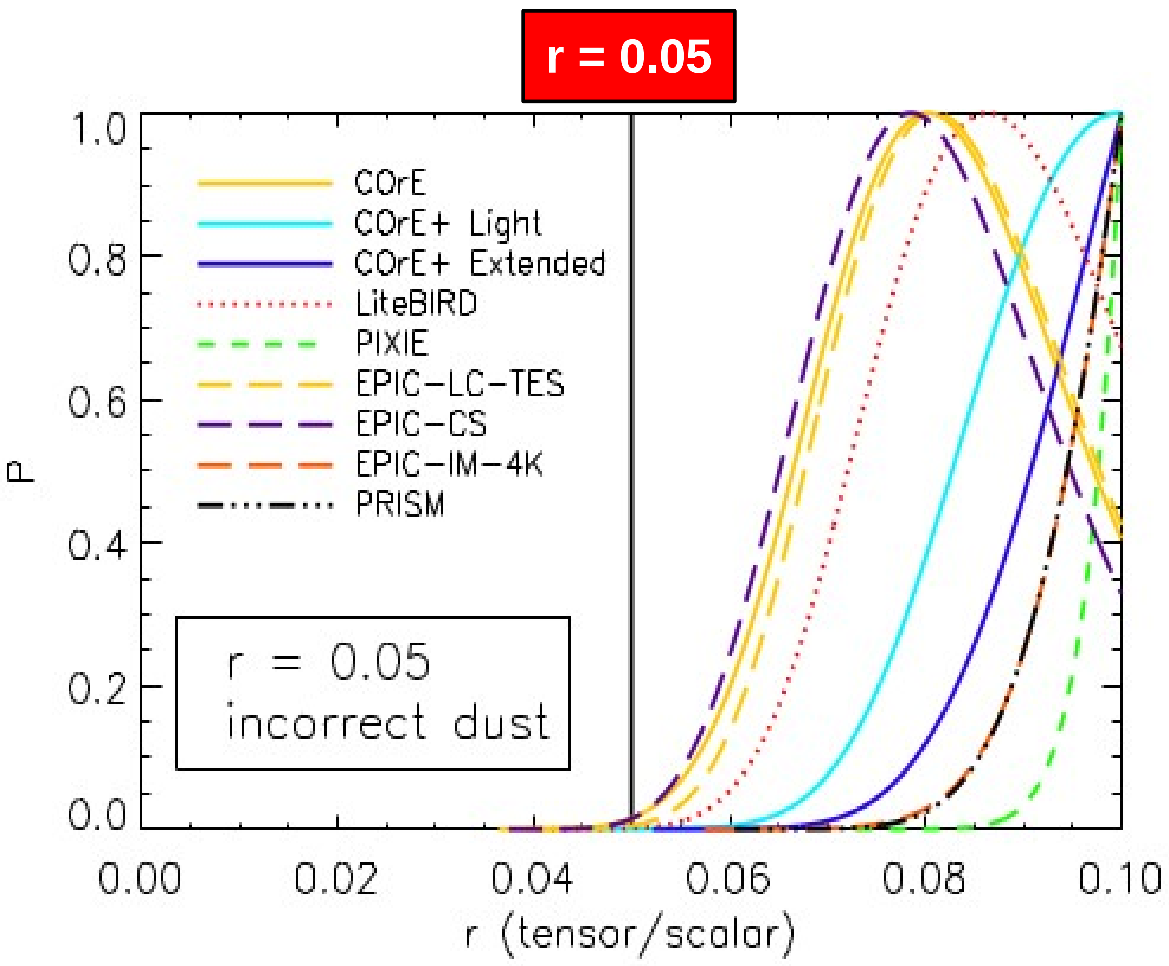

Incorrect spectral modelling of thermal dust strongly bias the most sensitive experiments

$\ell_{max} \sim 12$

χ^2	r	
1.07	0.08929 ± 0.00766	COrE+ Light
1.20	0.09218 ± 0.00624	COrE+ Extended
1.12	0.08023 ± 0.01045	COrE
1.10	0.08428 ± 0.00935	LiteBIRD
1.08	0.09711 ± 0.00265	PIXIE
1.32	0.08113 ± 0.00999	EPIC-LC-TES
1.08	0.07911 ± 0.01048	EPIC-CS
2.88	0.09434 ± 0.00485	EPIC-IM-4K
1.58	0.09446 ± 0.00467	PRISM

7σ bias

4σ bias

Remazeilles, Dickinson, Eriksen, Wehus, MNRAS 2016

Impact of mismodelling synchrotron : neglecting index curvature

r = 0.05

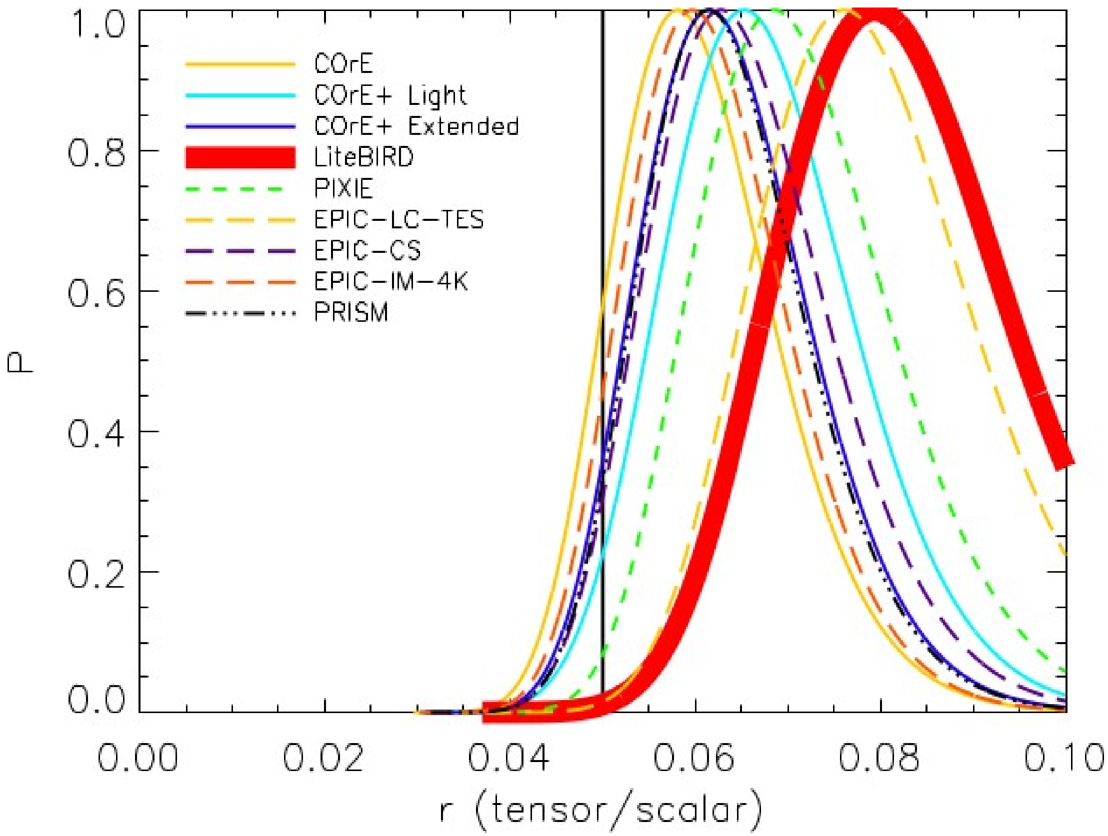

LiteBIRD original

χ^2	r	
1.00	0.06756 ± 0.01027	COrE+ Light
1.01	0.06390 ± 0.00946	COrE+ Extended
1.01	0.06074 ± 0.00920	COrE
1.01	0.07988 ± 0.01027	LiteBIRD
1.01	0.07122 ± 0.01027	PIXIE
1.09	0.07769 ± 0.01029	EPIC-LC-TES
0.99	0.06558 ± 0.01004	EPIC-CS
1.30	0.06205 ± 0.00906	EPIC-IM-4K
1.12	0.06386 ± 0.00925	PRISM

extra bias: false r detection with no χ^2 evidence !

→ lack of low-frequency channels

Remazeilles, Dickinson, Eriksen, Wehus, MNRAS 2016

Why do we need extra frequencies?

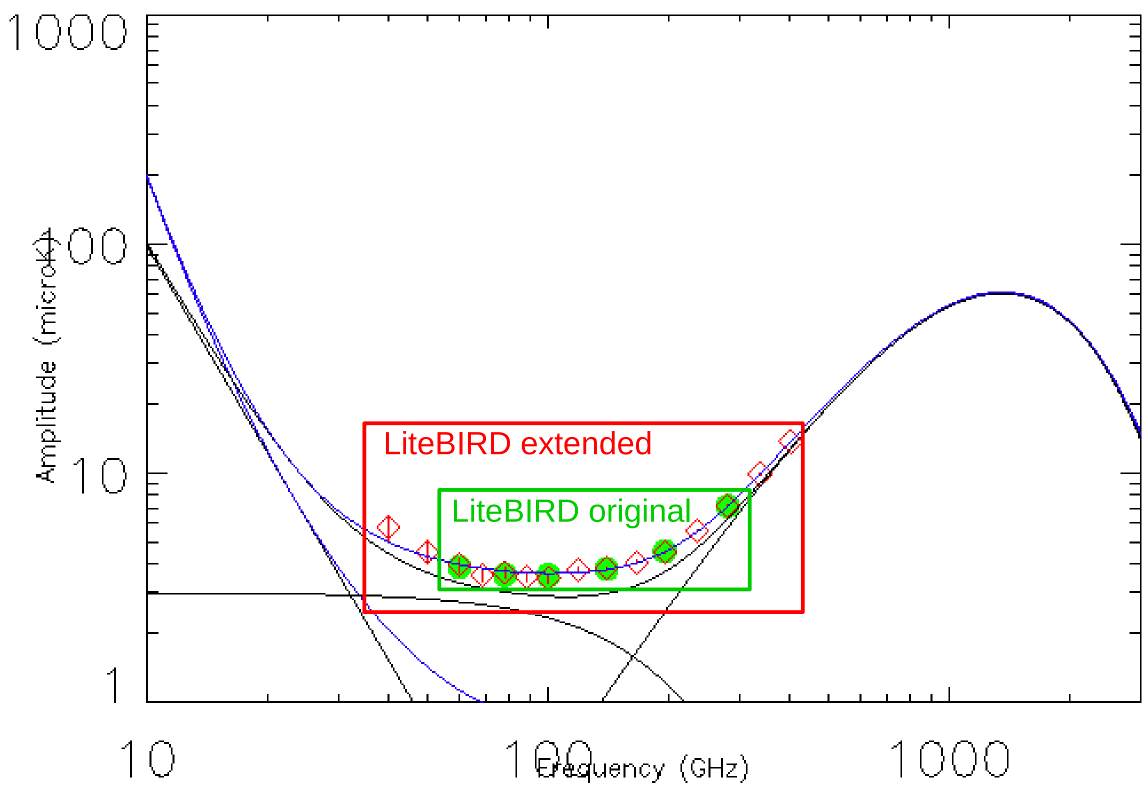

Index curvature can make synchrotron spectrum less “orthogonal” to CMB spectrum

Over a restricted frequency range, spectral flattening may prevent component separation techniques from distinguishing between CMB and synchrotron B-modes

i.e., the global sky is correctly fitted ($\chi^2 \sim 1$) but individual synchrotron and CMB components are not correctly splitted (r is biased)

Impact of mismodelling synchrotron : neglecting index curvature

r = 0.05

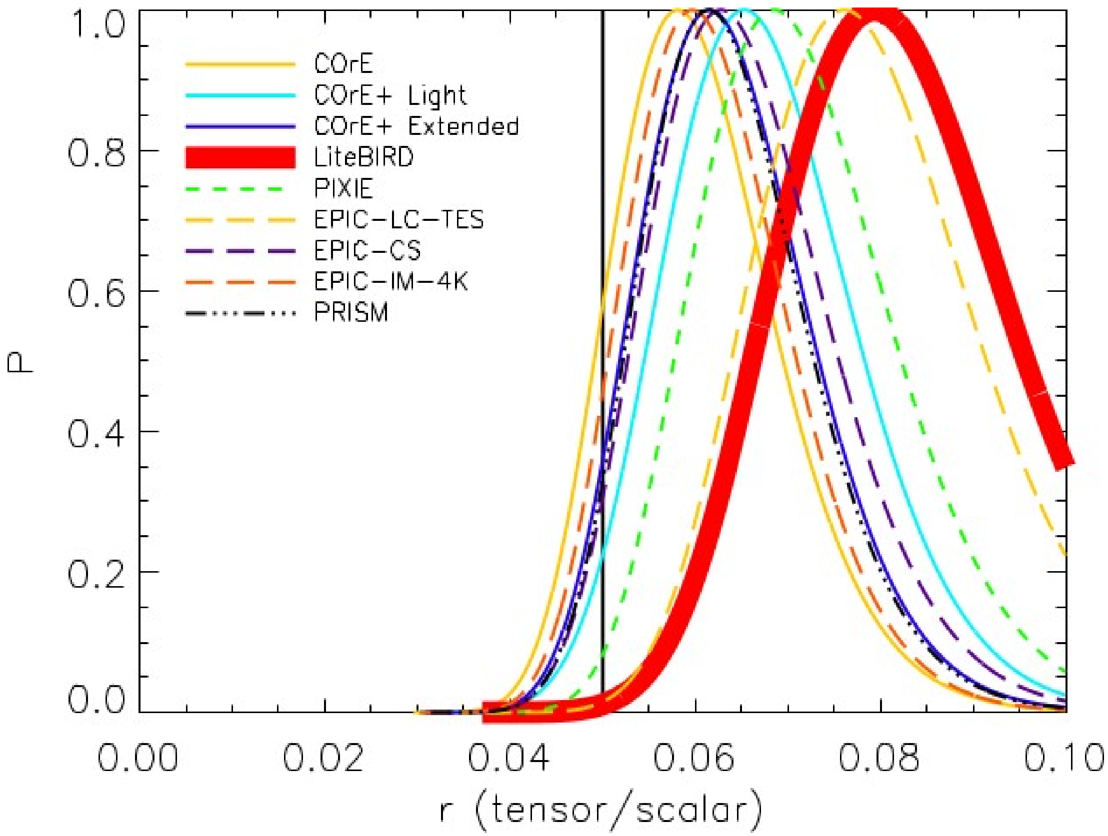

LiteBIRD original

Remazeilles, Dickinson, Eriksen, Wehus, MNRAS 2016

Impact of mismodelling synchrotron : neglecting index curvature

r = 0.05

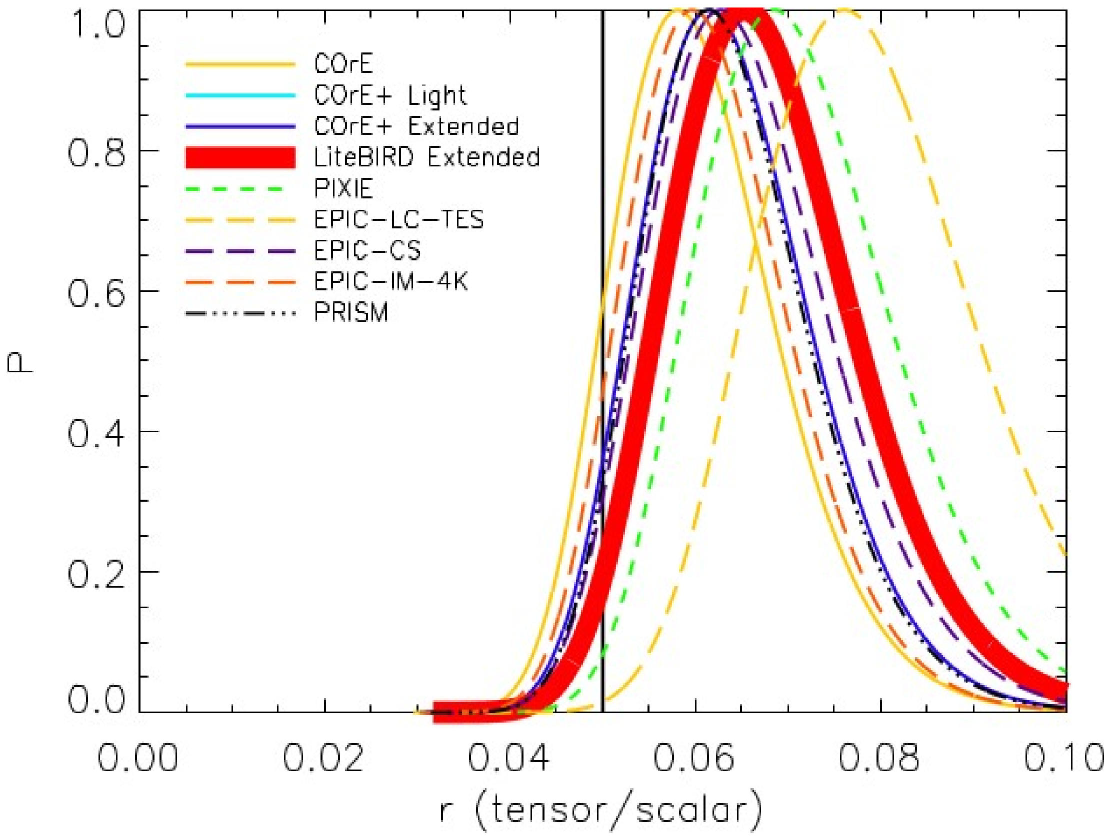

LiteBIRD extended

Remazeilles, Dickinson, Eriksen, Wehus, MNRAS 2016

Splitting tensor and lensing B-modes

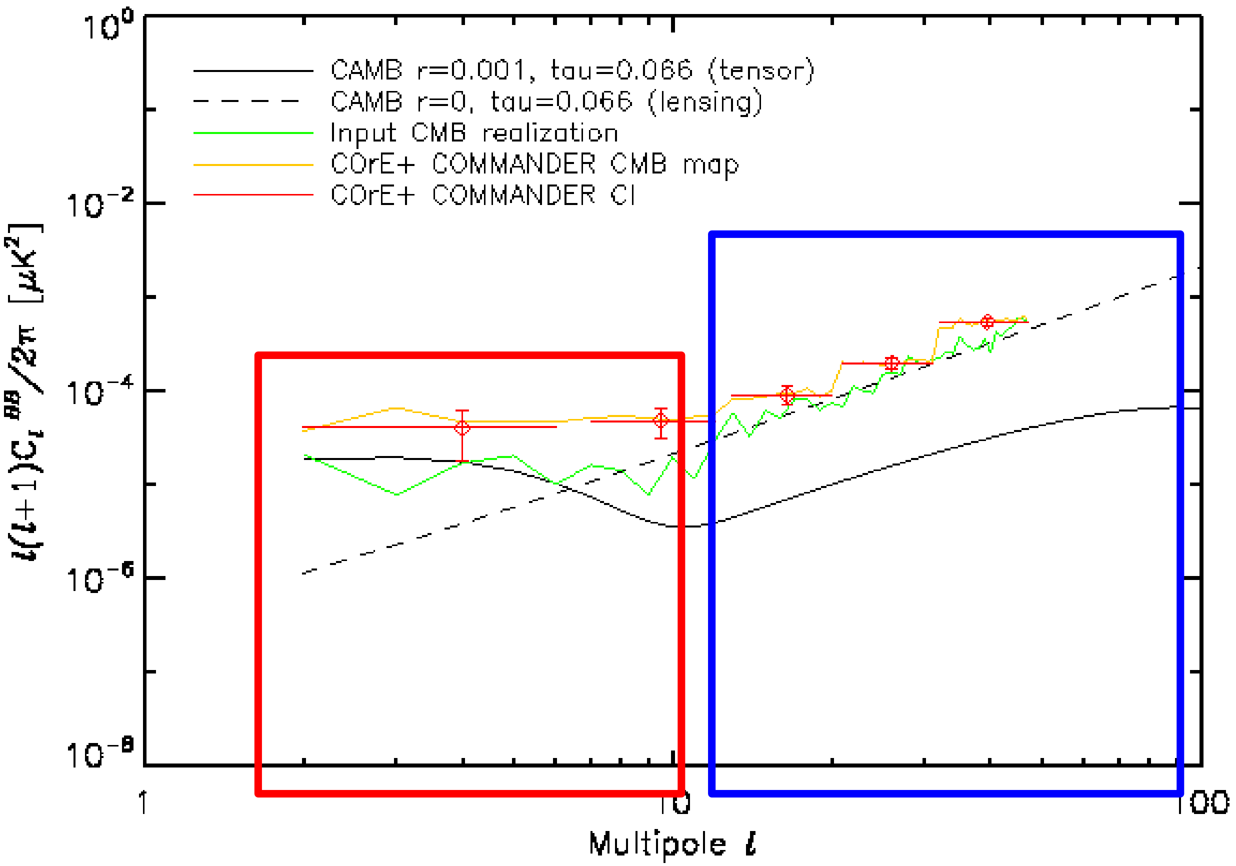

- We do need to control foregrounds at $\ell < 12$ (reionization peak) to disentangle tensor B-modes and lensing B-modes !
- Detecting the reionization peak is a must-have when we claim for a satellite mission

COMMANDER methodology

1. Separation of components (MCMC Gibbs sampling)

$\boldsymbol{s}^{(i+1)} \leftarrow P\left(\boldsymbol{s} \middle| C_\ell^{(i)}, \boldsymbol{\beta}^{(i)}, \boldsymbol{d}\right),$	amplitudes
$C_\ell^{(i+1)} \leftarrow P\left(C_\ell \middle| \boldsymbol{s}^{(i+1)}\right),$	CMB power spectrum
$\boldsymbol{\beta}^{(i+1)} \leftarrow P\left(\boldsymbol{\beta} \middle| \boldsymbol{s}^{(i+1)}, \boldsymbol{d}\right),$	spectral indices

2. Likelihood estimation of r and A_{lens} :

$$-2\ln\mathcal{L}\left[\widehat{C}_\ell | C_\ell^{th}\left(r, A_{lens}\right)\right] = \sum_\ell (2\ell+1)\left[\ln\left(\frac{C_\ell^{th}}{\widehat{C}_\ell}\right) + \frac{C_\ell^{th}}{\widehat{C}_\ell} - 1\right]$$

$$C_\ell^{th} = r\, C_\ell^{tensor}(r=1) + A_{lens}\, C_\ell^{lensing}(r=0).$$

Remazeilles, Dickinson, et al, in prep. (2016)

Correct for lensing bias if not variance

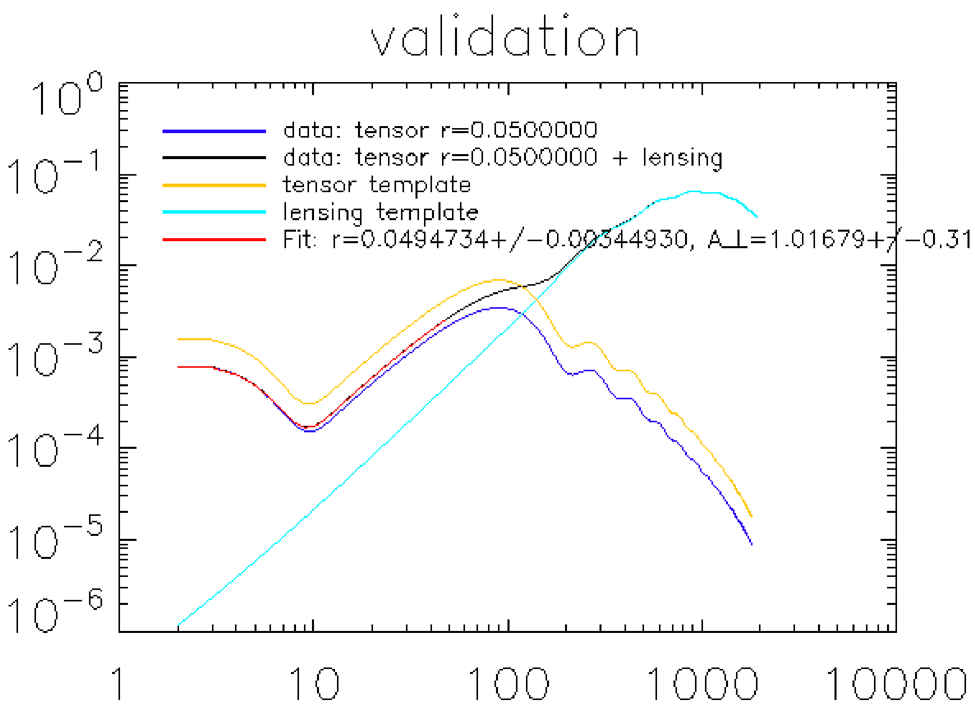

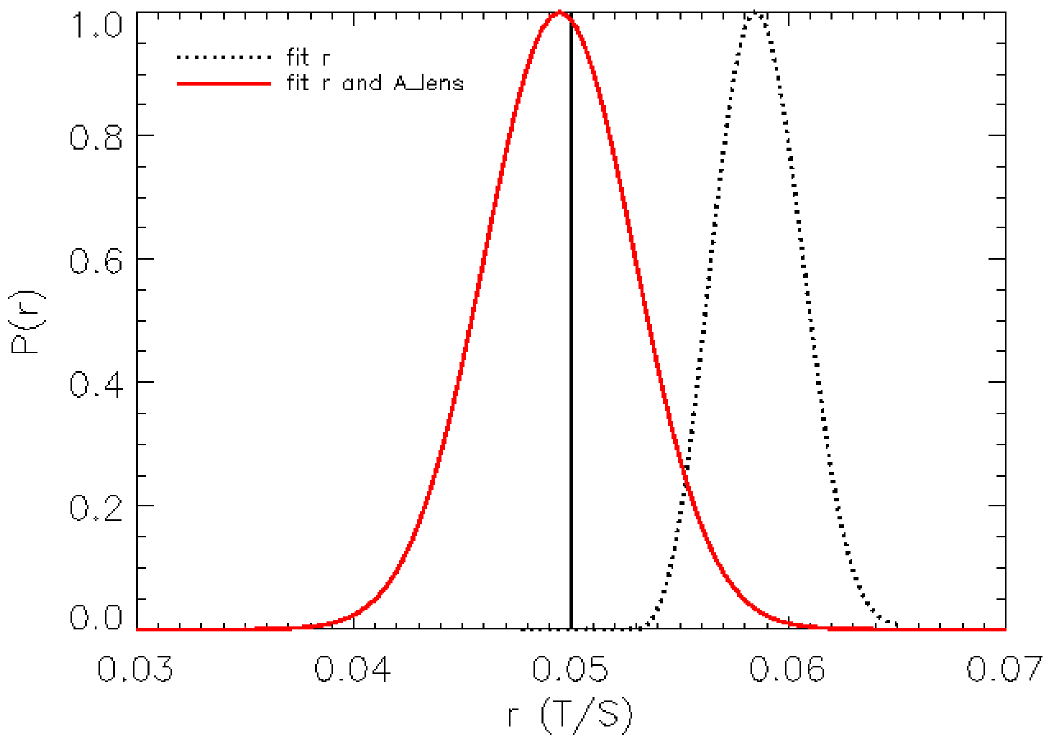

Remazeilles, Dickinson, et al, in prep. (2016)

Variance cost of “delensing” the power spectrum

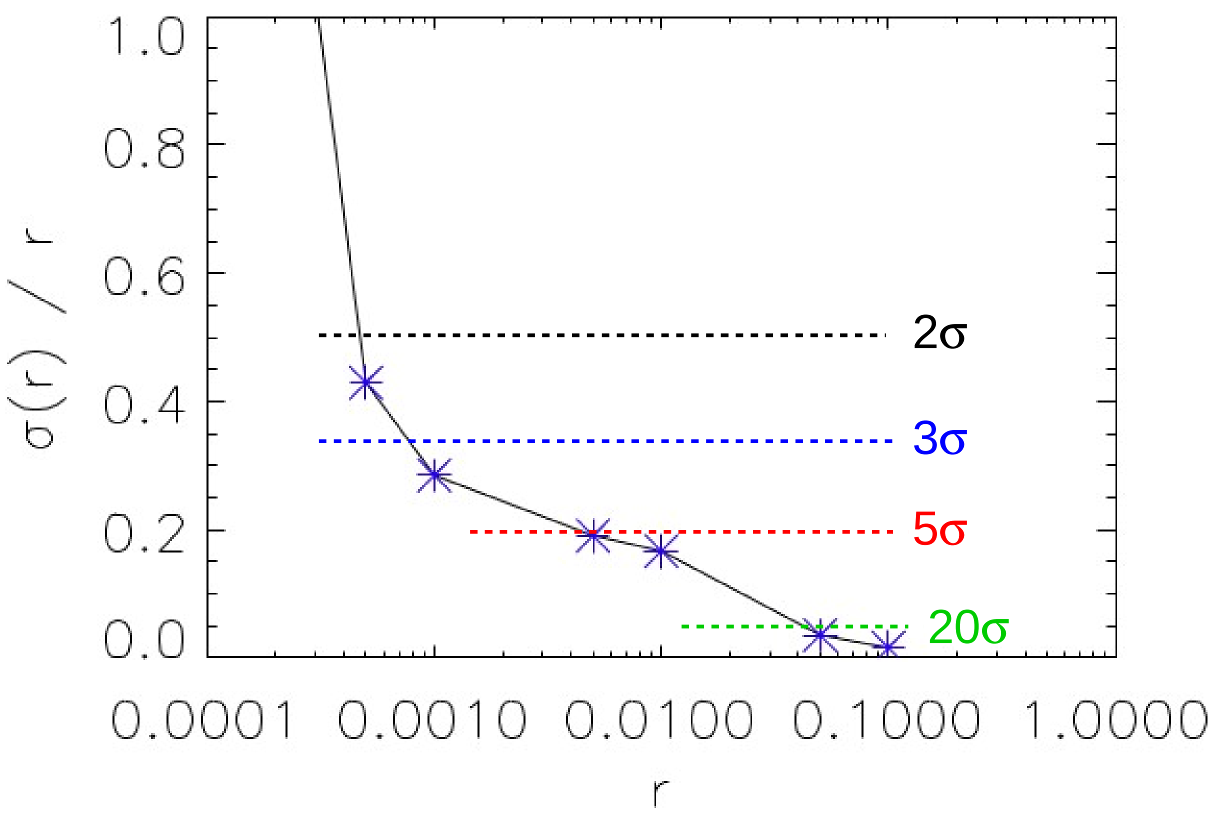

Remazeilles, Dickinson, et al, in prep. (2016)

Backup slides

CMB B-mode polarization satellite concepts

Concept name	Leading country/ institution	Frequencies [GHz]	Beam size FWHM [arcmin]	Sensitivities [μK deg]	Reference/notes
EPIC-LC-TES	U.S.A. (NASA)	30,40,60,90 135,200,300	155,116,77,52, 34,23,16	0.460,0.156,0.085,0.037, 0.035,0.037,0.062	EPIC Low-Cost option with TES detectors (Bock et al. 2008)
EPIC-CS	U.S.A. (NASA)	30,45,70,100, 150,220,340,500	15.5,10.3,6.6,4.6, 3.1,2.1,1.4,0.9	0.683,0.367,0.150,0.117 0.117,0.183,0.883,7.50	EPIC Comprehensive-Science option (Bock et al. 2008)
EPIC-IM-4K	U.S.A. (NASA)	30,45,70,100,150 220,340,500,850	28,19,12,8.4,5.6 3.8,2.5,1.7,1.0	0.147,0.061,0.027,0.018,0.014, 0.027,0.058,0.014,0.012	EPIC Intermediate with 4 K mirror (Bock et al. 2009)
LiteBIRD	Japan (JAXA)	60,78,100, 140,195,280	75,58,45, 32,24,16	0.172,0.108,0.078, 0.062,0.0517,0.063	(Matsumura et al. 2013)
COrE	Europe (ESA)	45,75,105,135,165, 195,225,255,285,315, 375,435,555,675,795	23.3,14,10,7.8,6.4, 5.4,4.7,4.1,3.7,3.3, 2.8,2.4,1.9,1.6,1.3	0.150,0.078,0.077,0.075,0.077 0.075,0.075,0.173,0.283,0.767, 1.95,4.25,9.82,57.0,348.0	ESA M mission concept (The COrE Collaboration et al. 2011)
COrE+ Light	Europe (ESA)	60,70,80,90,100, 115,130,145,160,175, 195,220,255,295,340, 390,450,520,600	21.0,18.0,15.8,14.0,12.6, 11.0,9.7,8.7,7.9,7.2, 6.5,5.7,5.0,4.3,3.7, 3.2,2.8,2.4,2.1	0.485,0.467,0.320,0.257,0.197, 0.138,0.110,0.092,0.092,0.090, 0.090,0.135,0.218,0.430,0.817, 1.645,4.205,10.535,15.848	ESA M mission concept 3[1]
COrE+ Extended	Europe (ESA)	60,70,80,90,100, 115,130,145,160,175, 195,220,255,295,340, 390,450,520,600,700,800	14.0,12.0,10.5,9.3,8.4, 7.3,6.5,5.8,5.3,4.8, 4.3,3.8,3.3,2.9,2.5, 2.2,1.9,1.6,1.4,1.2, 1.1	0.342,0.233,0.160,0.123,0.098, 0.073,0.057,0.057,0.057,0.058, 0.063,0.090,0.152,0.220,0.422, 0.790,1.982,5.632,20.05,93.5,203	ESA M mission concept 4[1]
PRISM	Europe (ESA)	30,36,43,51,62, 75,90,105,135,160, 185,200,220,265,300, 320,395,460,555,660	17,14,12,10,8.2, 6.8,5.7,4.8,3.8,3.2 2.8,2.5,2.3,1.9,1.7, 1.6,1.3,1.1,0.92,0.77	0.211,0.141,0.133,0.103,0.098, 0.093,0.078,0.068,0.061,0.0572 0.059,0.061,0.064,0.073,0.085, 0.092,0.135,0.197,0.404,0.953	ESA L mission concept (André et al. 2014)
PIXIE	U.S.A. (NASA)	30,60,90,120,150, 180,210,240,270,300, 330,360,390,420,450, 480,510,540,570,600, 630,660,690,720,750, 780,810,840,870,900, 930,960,990,1020,1050, 1080,1110,1140,1170,1200	96.0 (constant)	5.180,1.390,0.691,0.454,0.352, 0.307,0.292,0.297,0.319,0.358 0.418,0.503,0.623,0.790,1.020, 1.350,1.800,2.440,3.350,4.660, 6.550,9.280,13.30,19.10,27.70, 40.50,59.60,88.20,131.00,196.00, 294.00,444.00,672.00,1020,1560, 2390,3670,5660,8750,13600	(Kogut et al. 2011)

Incorrect dust modelling : impact of high frequency channels

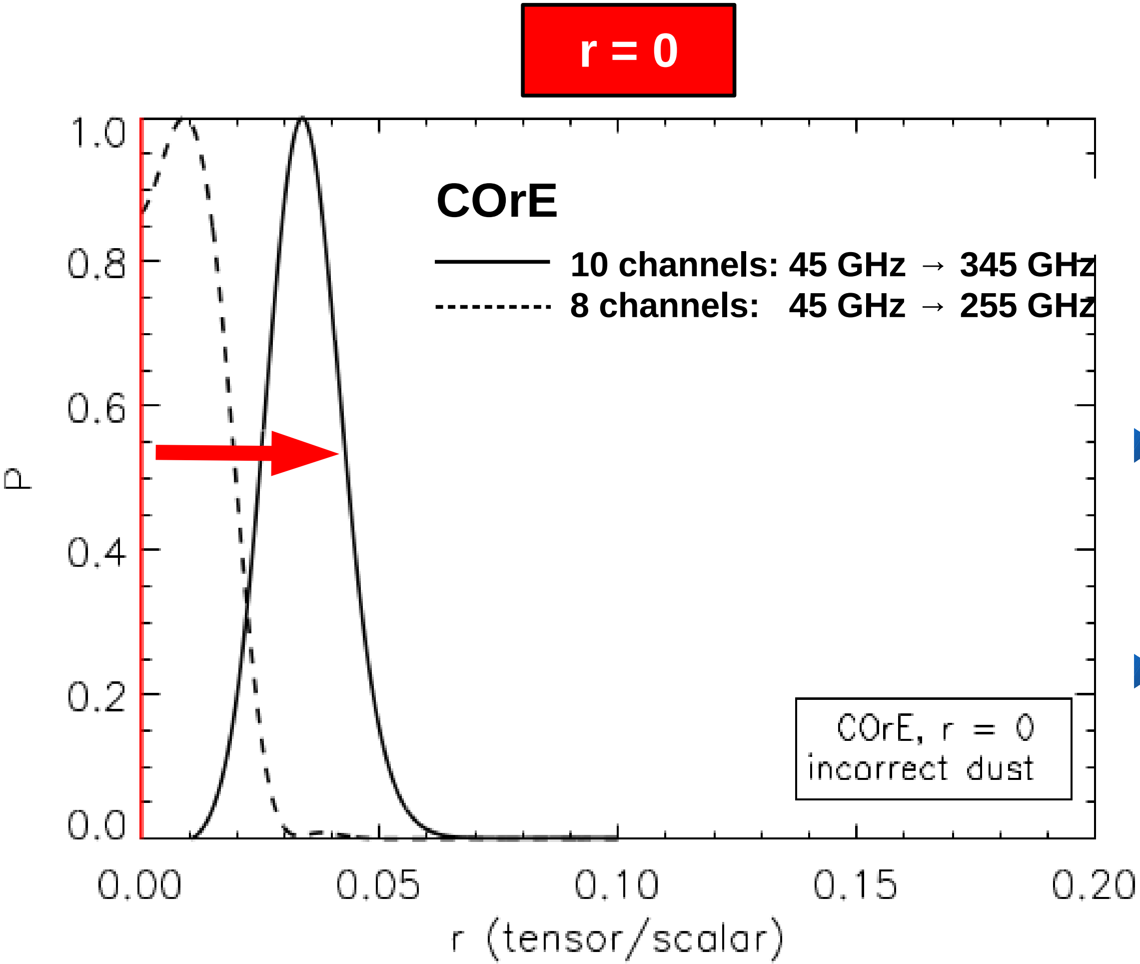

- ***High-frequency channels useful to highlight any failure in the model of polarized dust***
- *Instability of P(r) distribution with respect to frequencies highlights spurious detection of dust B-modes*

Remazeilles, Dickinson, Eriksen, Wehus, MNRAS 2016

Incorrect dust modelling : impact of Galactic masking

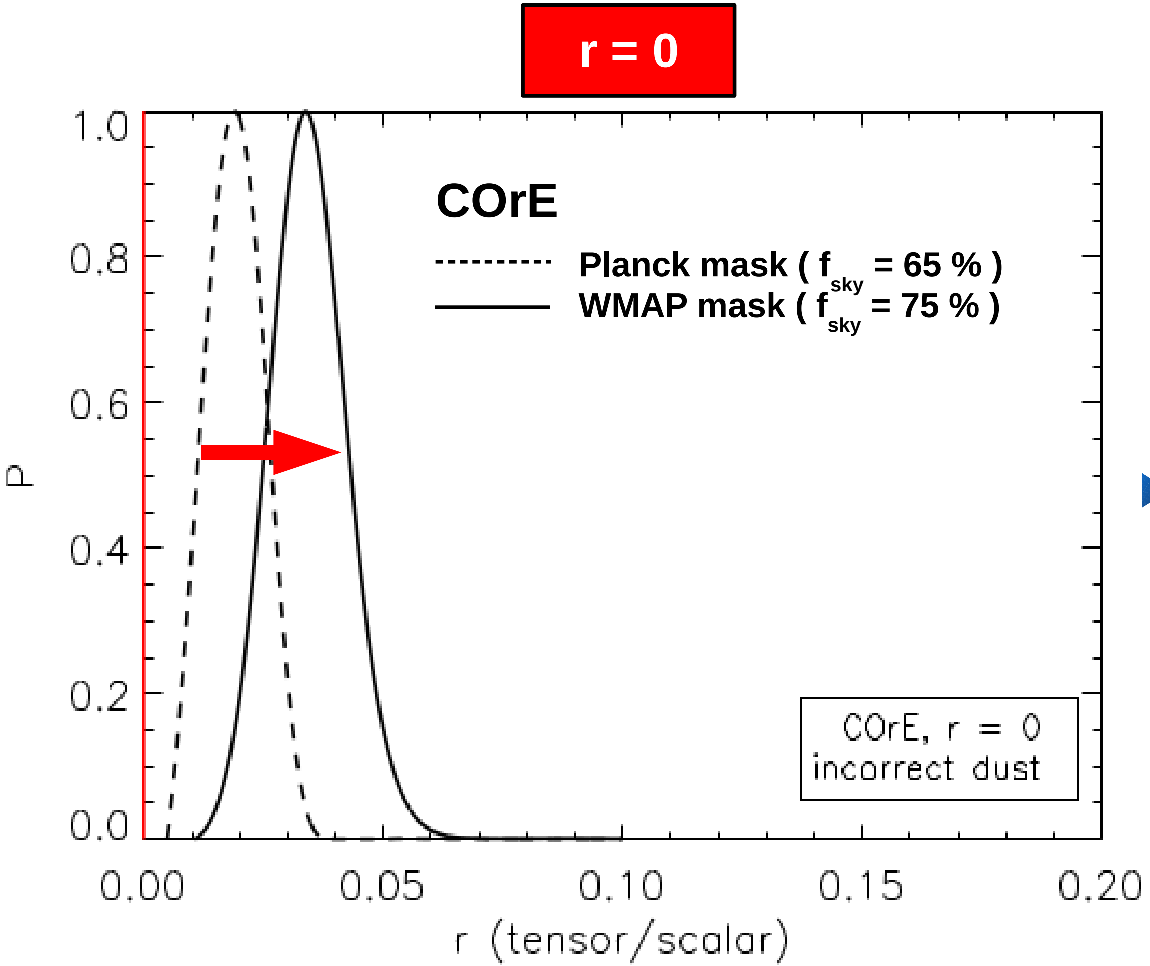

- *Instability of P(r) distribution with respect to the size of the mask highlights spurious detection of dust B-modes*

Remazeilles, Dickinson, Eriksen, Wehus, MNRAS 2016

MCMC Gibbs sampling

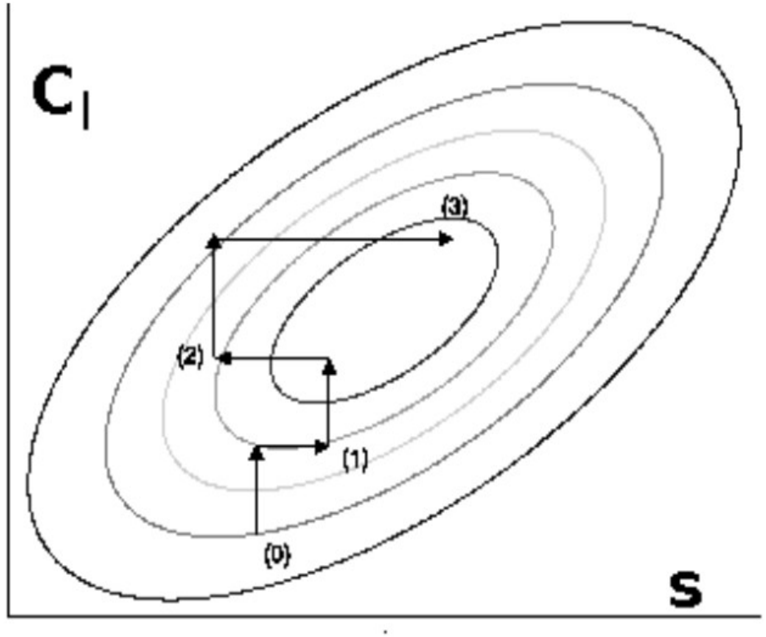

$$\boldsymbol{s}^{(i+1)} \leftarrow P\left(\boldsymbol{s} \middle| C_\ell^{(i)}, \boldsymbol{d}\right)$$

$$C_\ell^{(i+1)} \leftarrow P\left(C_\ell \middle| \boldsymbol{s}^{(i+1)}, \boldsymbol{d}\right)$$

C_ℓ sampling

$$P\left(C_\ell \middle| \boldsymbol{s}, \boldsymbol{d}\right) = P\left(C_\ell \middle| \boldsymbol{s}\right) \propto \frac{e^{-\frac{(2\ell+1)}{2C_\ell}\left(\frac{1}{2l+1}\sum_{m=-\ell}^{\ell}|\boldsymbol{s}_{\ell m}|^2\right)}}{C_\ell^{(2\ell+1)/2}}$$

- Inverse-Gamma distribution
- Simple textbook sampling algorithm $\rightarrow C_\ell^{(i+1)}$

Amplitude sampling

$$P\left(\boldsymbol{s}\middle|C_\ell, \boldsymbol{d}\right) \propto P\left(\boldsymbol{d}\middle|\boldsymbol{s}, C_\ell\right) P\left(\boldsymbol{s}\middle|C_\ell\right)$$
$$\propto e^{(-1/2)(\boldsymbol{d}-\boldsymbol{s})^T \boldsymbol{N}^{-1}(\boldsymbol{d}-\boldsymbol{s})} e^{(-1/2)\boldsymbol{s}^T \boldsymbol{S}^{-1}\boldsymbol{s}}$$
$$\propto e^{(-1/2)(\boldsymbol{s}-\widehat{\boldsymbol{s}})^T\left(\boldsymbol{S}^{-1}+\boldsymbol{N}^{-1}\right)(\boldsymbol{s}-\widehat{\boldsymbol{s}})}$$

- Gaussian distribution where $\widehat{\boldsymbol{s}} = \left(\boldsymbol{S}^{-1} + \boldsymbol{N}^{-1}\right)^{-1} \boldsymbol{N}^{-1}\boldsymbol{d}$ is the Wiener
- $\boldsymbol{s}^{(i+1)}$ is solution (conjugate gradients) of

$$\left(\boldsymbol{S}^{-1} + \boldsymbol{N}^{-1}\right)\boldsymbol{s} = \boldsymbol{N}^{-1}\boldsymbol{d} + \boldsymbol{S}^{-1/2}w_0 + \boldsymbol{N}^{-1/2}w_1$$

where $w_0, w_1 \sim \mathcal{N}(0, 1)$